Nonmonotonic Behavior in Hydrogen Production from the Steam Reforming of Higher Hydrocarbons in a Circulating Fluidized Bed Membrane Reformer

Zhongxiang Chen,* Yibin Yan, and Said S. E. H. Elnashaie

Department of Chemical Engineering, Auburn University, Auburn, Alabama 36849-5127

The nonmonotonic behavior observed in hydrogen production from the steam reforming of higher hydrocarbons over nickel catalyst in an earlier-suggested novel circulating fast fluidized bed membrane reformer (CFFBMR) (Chen et al. *AIChE J*. **2003**, *49* (5), 1250−1265) is extensively investigated. The investigation is carried out using kinetic model simulation at 623−823 K and 1013 kPa. Hydrogen-permselective membranes are used under cocurrent and countercurrent operations. The results show that the yield of hydrogen decreases at 623−723 K and then increases at 723−823 K. At 623 K, heptane is not fully converted, and thermodynamic equilibrium is not established. In contrast at 723−823 K, heptane is fully converted, and thermodynamic equilibrium is established. The strong methanation reaction at 723 K makes the hydrogen yield much lower, whereas at 823 K, the steam reforming of methane becomes increasingly important, enhancing the production of hydrogen. Using hydrogen-permselective membranes, the thermodynamic equilibrium limitation is "broken", and the CFFBMR performance is significantly improved. However, because of the small or negative driving force for hydrogen permeation under cocurrent operation, the hydrogen yield at 723 K is still lower. To improve this process, countercurrent operation is further investigated and found to be more efficient for hydrogen production when hydrogen-permselective membranes are used at 723−823 K. The purity of the exit hydrogen in the membranes is 90.65 and 92.83 mol % for cocurrent and countercurrent operations, respectively, at 823 K. If the sweep gas steam is further condensed, the purity of hydrogen could be as high as 99.45 and 99.59 mol %, respectively.

Introduction

Hydrogen is often rightly called the perfect fuel, and it is mostly produced from the steam reforming of hydrocarbons.[1−6] Steam reforming not only extracts the hydrogen from hydrocarbons, but also extracts the hydrogen from water. One of the major benefits of this technique is that the reserve of water on earth is virtually inexhaustible. Steam reforming of natural gas, mainly methane, has been widely studied in different reactor configurations.[4,7−15] However, the feedstock for hydrogen production varies from place to place because of the availability of hydrocarbons.[2,16] Recent years have shown progress in steam reforming technology, resulting in cheaper plants and higher feedstock flexibility because of the better materials used for reforming reactors, better control of coking, and better reforming catalysts.[17] Steam reforming of higher hydrocarbons is of great importance for hydrogen production not only as a novel fuel, but also in the traditional chemical and petrochemical industries.[3,16,18−21] Usually, steam reforming of higher hydrocarbons can be represented by the following reactions[3]

$$C_nH_m + nH_2O \rightarrow nCO + \left(n + \frac{m}{2}\right)H_2$$
(for heptane, $n = 7$, $\Delta H° = 1108$ kJ/mol) (1)

$$CO + 3H_2 \rightleftharpoons CH_4 + H_2O \qquad (\Delta H° = -206.2 \text{ kJ/mol}) \tag{2}$$

$$CO + H_2O \rightleftharpoons CO_2 + H_2 \qquad (\Delta H° = -41.2 \text{ kJ/mol}) \tag{3}$$

Because of the generation of methane by the methanation reaction (eq 2), steam reforming of methane also takes place in the steam reformer. The higher hydrocarbons are irreversibly converted into carbon monoxide and hydrogen, followed by the fast methanation reaction (eq 2) and water−gas shift reaction (eq 3). An industrial steam reformer typically consists of a fixed bed made up of a large number of catalyst tubes, surrounded by a huge top-/side-fired furnace.[22] Chen et al.[1] recently outlined the advantages of using a recent proposed novel circulating fast fluidized bed membrane reformer (CFFBMR) for the steam reforming of higher hydrocarbons. They investigated the effects of reaction conditions, including reaction temperature, steam-to-carbon feed ratio, reaction pressure, heating policies, and oxygen introduction method (by direct feed and/or through oxygen-permeable membranes), on the membrane reformer performance for the cases with and without hydrogen and/or oxygen permselective membranes. On the basis of these preliminary investigations, parameter optimization was carried out. In this paper, an interesting phenomenon that the yield of hydrogen is nonmonotonic with respect to the reaction temperature in this novel proposed circulating fast fluidized bed membrane reformer is extensively studied using kinetics models for cocurrent and countercurrent operations. This paper mainly focuses on the reaction characteristics, thermo-

* To whom correspondence should be addressed. E-mail: chenzho@auburn.edu. Tel.: 1-334-844-2051. Fax: 1-334-844-2063.

10.1021/ie021013j CCC: $25.00
Published on Web 10/30/2003

Table 1. Reaction Kinetics and Parameters

Kinetic Equations

reaction	kinetic rate equation	ref
$C_7H_{16} + 7H_2O \rightarrow 7CO + 15H_2$	$r_1 = \dfrac{k_1 P_{C_7H_{16}}}{\left[1 + K_a\left(\dfrac{P_{C_7H_{16}} P_{H_2}}{P_{H_2O}}\right) + K_b\left(\dfrac{P_{H_2O}}{P_{H_2}}\right)\right]^2}$	21
$CH_4 + H_2O \rightleftharpoons CO + 3H_2$	$r_2 = k_2\left(\dfrac{P_{CH_4} P_{H_2O}}{P_{H_2}^{2.5}} - \dfrac{P_{CO} P_{H_2}^{0.5}}{K_2}\right)/\mathrm{DEN}^2$	23
$CO + H_2O \rightleftharpoons CO_2 + H_2$	$r_3 = k_3\left(\dfrac{P_{CO} P_{H_2O}}{P_{H_2}} - \dfrac{P_{CO_2}}{K_3}\right)/\mathrm{DEN}^2$	23
$CH_4 + 2H_2O \rightleftharpoons CO_2 + 4H_2$	$r_4 = k_4\left(\dfrac{P_{CH_4} P_{H_2O}^2}{P_{H_2}^{3.5}} - \dfrac{P_{CO_2} P_{H_2}^{0.5}}{K_2 K_3}\right)/\mathrm{DEN}^2$	23
	$\mathrm{DEN} = 1 + K_{CO}P_{CO} + K_{H_2}P_{H_2} + K_{CH_4}P_{CH_4} + K_{H_2}OP_{H_2}O/P_{H_2}$	

Reaction Rate Constants

rate constant	preexponential factor	activation energy and heat of chemisorption (kJ/mol)
k_1 [kmol/(kPa kg_{cat} h)]	8×10^5	67.8
k_2 [kmol/(kg_{cat} h kPa)]	9.49×10^{16}	240.1
k_3 [(kmol $kPa^{0.5}$)/(kg_{cat} h)]	4.39×10^4	67.13
k_4 [(kmol $kPa^{0.5}$)/(kg_{cat} h)]	2.29×10^{16}	243.9
K_a (kPa^{-1})	25.2	–
K_b	0.077	–
K_{CH_4} (kPa^{-1})	6.65×10^{-6}	38.28
K_{CO} (kPa^{-1})	8.23×10^{-7}	70.65
K_{H_2O}	1.77×10^5	-88.68
K_{H_2} (kPa^{-1})	6.12×10^{-11}	82.9

Reaction Equilibrium Constants

equilibrium constant	expression
K_1 (kPa^2)	$100e^{-26830/T+30.114}$
K_2	$e^{4400/T-4.036}$

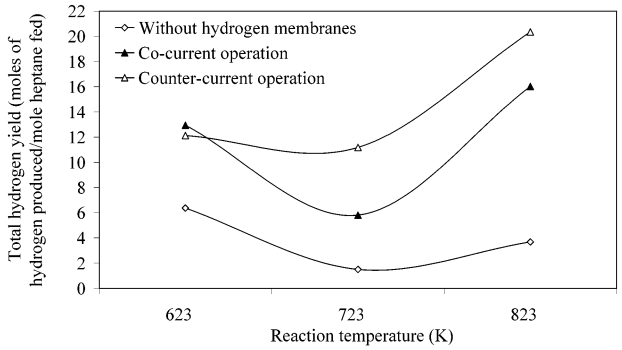

Figure 1. Nonmonotonic behavior in hydrogen production with respect to the reaction temperature in the CFFBMR.

dynamic equilibrium, and driving force for hydrogen permeation between the reaction side and membrane side. Figure 1 shows this nonmonotonic behavior. Only hydrogen-permeable membranes are used for this investigation. Countercurrent operation provides a more promising engineering method to improve the production of hydrogen.

Reaction Scheme and Kinetics

Earlier results have shown that, under typical operating conditions, the steam reforming of higher hydrocarbons is irreversible and the methanation and water–gas shift reactions rapidly approach equilibrium.[3,16,18–21] In studies of the steam reforming of higher hydrocarbons, heptane is usually used as a model hydrocarbon.[3,20,21] As mentioned earlier, the product mixture is initially rich with methane. Steam reforming of methane takes place, and the kinetics of this reaction is also considered in the overall system. Table 1 summarizes the reactions kinetics and parameters for the steam reforming of heptane and byproduct methane on a nickel reforming catalyst. For the kinetics of the steam reforming of heptane, Tottrup directly applied the intrinsic rate equation (first equation in Table 1) for industrial steam reformers and found good agreement between the experimental and calculated data.[21] For the kinetics of the steam reforming of methane, Elnashaie et al. analyzed this set of kinetic rate equations and found it to be the most general rate equations.[22,24] They also found that the rate of methane steam reforming is nonmonotonic with respect to the partial pressure of steam.[24]

Mathematical Modeling

In the circulating fast fluidized bed membrane reformer, palladium-based hydrogen-permeable membranes are used. The product hydrogen permeates into the hydrogen membrane tubes as a result of the difference in the partial pressure of hydrogen and then is carried away by the sweep gas, steam. Two kinds of operation modes, cocurrent and countercurrent, between

Table 2. Mathematical Modeling Equations for Cocurrent and Countercurrent Operations

	Riser Reformer Reaction Side
component i	$\frac{dF_i}{dl} = \rho_{cat}A(1-\epsilon)\sum_{j=1}^{4}\sigma_{i,j}r_j - J_i\pi N_{H_2}d_{H_2}$
boundary condition	at $l = 0$, $F_i = F_{i0}$
	Hydrogen Permeation Side
hydrogen in the membrane tubes	$\frac{dF_{H_2}}{dl} = aJ_{H_2}\pi N_{H_2}d_{H_2}$ $a = \begin{cases} 1 & \text{cocurrent operation} \\ -1 & \text{countercurrent operation} \end{cases}$
sweep gas in the membrane tubes	$F_{SG} = F_{SG0} = \text{constant}$
boundary conditions	$\begin{cases} \text{at } l = 0 \quad F_{H_2,P} = F_{H_2,P0} = 0 & \text{cocurrent operation} \\ \text{at } l = L \quad F_{H_2,P} = F_{H_2,P0} = 0 & \text{countercurrent operation} \end{cases}$
hydrogen permeation flux	$J_{H_2} = Qe^{-E_{H2,P}/RT} / \delta_{H_2}(\sqrt{P_{H_2,r}} - \sqrt{P_{H_2,P}})$[27,28]
other component permeation fluxes ($i \neq H_2$)	$J_i = 0$

the reformer reaction side and membrane permeation side are investigated.

As described in an earlier paper,[1] the reactants and catalyst particles flow into the reformer, and the steam reforming reactions take place over the nickel reforming catalyst in this novel CFFBMR. In the circulating fluidization state, the velocity of the reactant mixture is sufficiently high (around 3 m/s) to carry the solid particles upward and out of the bed. The fraction of the solid particles is around 0.2 in the main reaction zone.[25,26] Because fine catalyst particles (mean size = 186 μm) are used in this CFFBMR, the slip between the solid and gas phases is assumed to be negligible. Because of the high circulation velocity of the gas and solid stream in the CFFBMR, the reformer is modeled as a plug-flow reactor (PFR). In the open literature, most of the reported data or models are related to fixed bed or bubbling fluidized bed steam reformers, which are usually called first- and second-generation steam reformers, respectively. This novel circulating fast fluidized bed membrane reformer is instead usually called a third-generation steam reformer. Starting with the elemental analysis for the material balance in the CFFBMR reaction side and hydrogen membrane side, one can derive a set of differential equations for cocurrent and countercurrent operations, as summarized in Table 2. The differential equations can be solved by integration using the stiff method of Gear or the backward differentiation formula with an automatic step size for high accuracy.[29] In this paper, the typical steam-to-carbon feed ratio is 2 mol/mol, and the reaction temperature is 623−823 K. Moreover, because of the continuous regeneration of the catalyst along the exit line of the reformer before recycling to the reformer, the effect of carbon deposition on catalyst deactivation is assumed to be negligible.

In Table 2, the mathematical modeling equations are almost the same for both cocurrent and countercurrent operations, except for the equation for the hydrogen permeation side, as shown regarding the sign of $a = \pm 1$. Under cocurrent operation, the concentration of hydrogen in the membrane side is zero at the entrance of the reformer, whereas under countercurrent operation, the concentration of hydrogen in the membrane side is the exit concentration of hydrogen at the entrance of the reformer. Therefore, the mathematical model equations for countercurrent operation are two-point boundary-value problems, which can be solved by using iterative or optimization techniques. Although, in a practical system for the steam reforming of higher hydrocarbons, the reformer is usually operated under nonisothermal conditions, to investigate the nonmonotonic behavior in hydrogen production with respect to the reaction temperature, we assume isothermal operation in the CFFBMR for this preliminary investigation. The results are still useful for other conditions, such as adiabatic and autothermal, because reaction temperature is a very important parameter for steam reforming systems.

Table 3. Reformer Construction Parameters and Reaction Conditions for CFFBMR

Construction Parameters for Reformer and Membrane Tubes		
length of reformer tube and membrane tubes		2 m
diameter of reformer tube		0.10 m
diameter of palladium-based hydrogen membrane tubes		0.005 m
thickness of palladium layer on hydrogen membrane tubes		20 μm
number of hydrogen membrane tubes		10
Nickel Reforming Catalyst		
shape of particles		spherical
diameter of catalyst particles		186 μm
solid catalyst density		2835 kg/m^3
solid fraction in the riser reformer		0.2
Process Gas Feed Rate		
riser reformer reaction side	component i	feed rate (mol/s)
	heptane	0.178
	steam	2.5
	hydrogen	0.0278
hydrogen membrane tubes	steam	0.278
Reaction Conditions		
temperature		623−823 K
pressure		1013 kPa
operating pressure in hydrogen membrane tubes		101.3 kPa
steam-to-carbon ratio (S/C)		2 mol/mol

Results and Discussion

The nonmonotonic behavior of hydrogen production with respect to the reaction temperature is investigated in the temperature range of 623−823 K. The main reformer construction parameters and reaction conditions are summarized in Table 3. The flow rate of hydrogen in the feed is not zero because there is a term in the kinetic rate equation for the steam reforming of heptane (first kinetic rate equation in Table 1) that requires division by the partial pressure of hydrogen. In the present work, the conversion of heptane is defined as the ratio of the converted amount of heptane to the

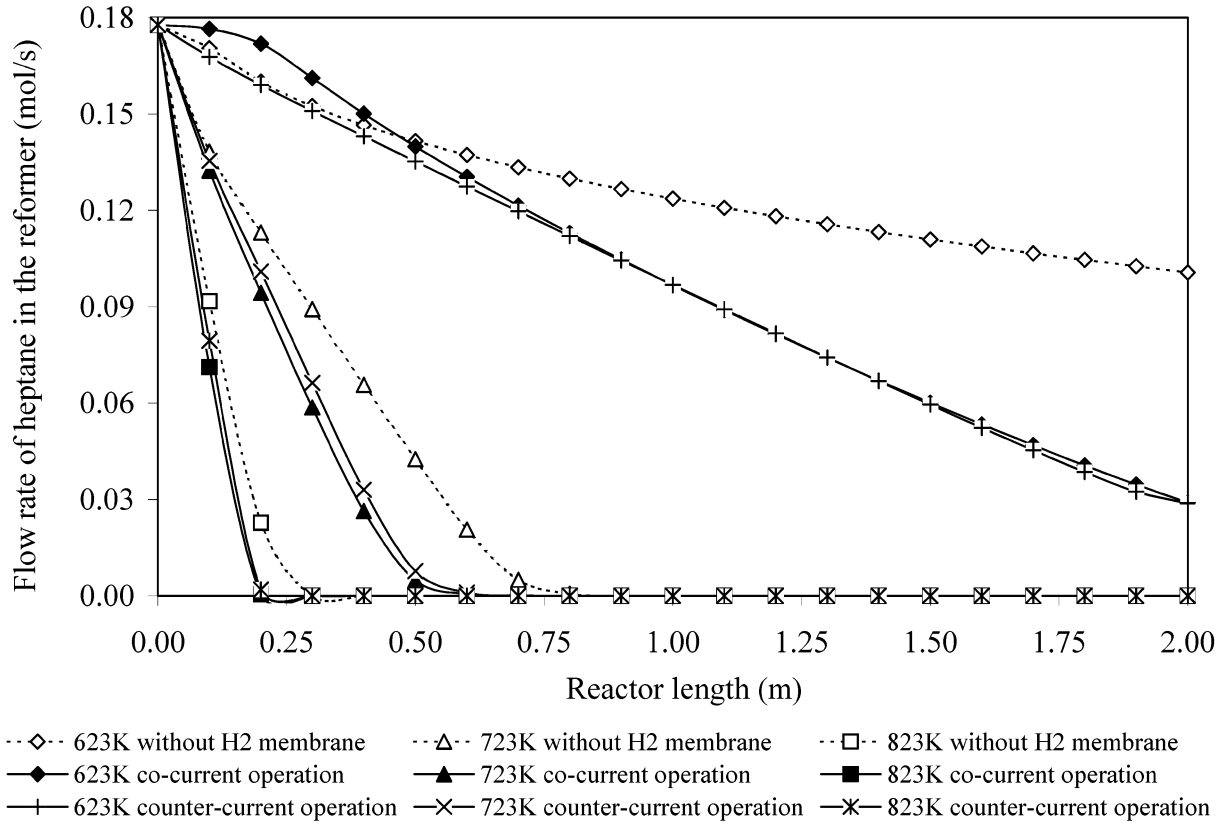

Figure 2. Flow rates of heptane at 623, 723, and 823 K for the three cases without any hydrogen membranes and cocurrent and countercurrent operations with 10 hydrogen membranes.

initial amount of heptane fed. The yields of hydrogen and methane are defined as the ratios of the amounts of product hydrogen and methane to the initial amount of heptane fed.

Isothermal CFFBMR Performance without Hydrogen-Selective Membranes. In this section the isothermal CFFBMR performance is studied at 623, 723 and 823 K without any palladium-based hydrogen-permselective membranes. The lowest curve in Figure 1 shows that the yield of hydrogen for this case is nonmonotonic with respect to the reaction temperature. At 623 K, the yield of hydrogen is 6.37 mol of hydrogen per mole of heptane fed, whereas at 723 and 823 K, the yields are 1.50 and 3.68 mol/mol, respectively. Figure 2 shows the flow rates of heptane in the reformer at 623, 723, and 823 K for the three cases of (a) no hydrogen membranes, (b) cocurrent operation with hydrogen membranes, and (c) countercurrent operation with hydrogen membranes. For the case without any hydrogen membranes, at the low temperature of 623 K, the flow rate of heptane in the reformer decreases along the reactor length, but it does not reach zero before exiting the CFFBMR. However, at the higher temperatures of 723 and 823 K, the flow rate of heptane at exit of the reformer is zero. Thus, heptane is fully converted in the reformer at 723 and 823 K. Figure 2 shows that the necessary reactor length for full heptane conversion is about 0.8 m for 723 K and 0.3 m for 823 K, which indicates that the steam reforming of heptane is a fast reaction at 723−823 K. Further investigation shows that thermodynamic equilibrium among the reversible methanation, methane steam reforming, and water−gas shift reactions is quickly established after the full conversion of heptane, resulting in a constant flow rate of methane along the rest of the reactor length (see Figure 3).

Accordingly, Table 4a shows the gas composition (mol %) at the exit of the CFFBMR reformer. As shown in Figure 2, heptane is not fully converted at 623 K. The main products in the reformer are hydrogen (31.25 mol %), carbon monoxide (11.19 mol %), and carbon dioxide (2.35 mol %). The concentration of methane in the exit gas stream is the lowest (1.01 mol %). The composition profile of product gases at 623 K implies that heptane steam reforming (first reaction in Table 1) is the dominant reaction in the system and the second most important reaction is the water−gas shift (third reaction in Table 1). In contrast, the methanation reaction (second reaction in Table 1) is not important at this low temperature, and therefore, steam reforming of the byproduct methane is negligible. Because hydrogen is continuously produced from the steam reforming of heptane at 623 K, thermodynamic equilibrium is not established among the reversible methanation, methane steam reforming, and water−gas shift reactions. However, at 723 and 823 K, heptane is fully converted (Figure 2), and then, a thermodynamic equilibrium state is rapidly established in the reformer, resulting in a constant flow rate of methane, as shown in Figure 3.

At 723 K, the main products in the reformer are methane (26.95 mol %), carbon dioxide (9.72 mol %), and hydrogen (8.7 mol %). Thus, at 723 K, the methanation reaction is the dominant reaction, which leads to a very high concentration of methane. Because 3 mol of hydrogen is consumed to produce 1 mol of methane via the methanation reaction, the higher the gas content of methane, the lower the gas content of hydrogen, and the lower the yield of hydrogen. At 723 K, the gas content of carbon dioxide is as high as 9.72 mol % in

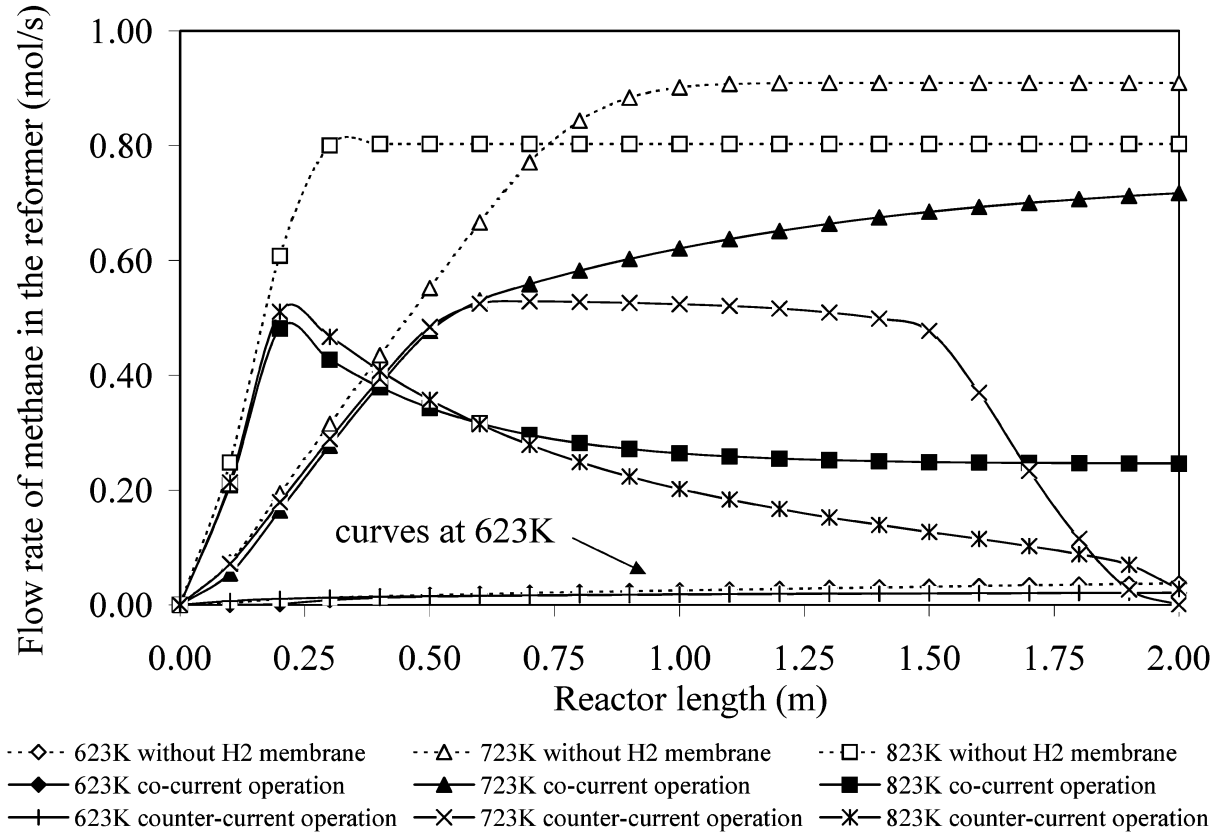

Figure 3. Flow rate of byproduct methane at 623, 723, and 823 K for the three cases without any hydrogen membranes and cocurrent and countercurrent operations with 10 hydrogen membranes.

Table 4. Exit Gas Composition (mol %) for the Cases without Any Hydrogen Membranes and Cocurrent and Countercurrent Operations with Hydrogen-Permeable Membranes

	(a) without membranes			(b) cocurrent operation with membranes			(c) countercurrent operation with membranes		
	623 K	723 K	823 K	623 K	723 K	823 K	623 K	723 K	823 K
C_7H_{16}	2.71	0.00	0.00	0.61	0.00	0.00	0.62	0.00	0.00
CH_4	1.01	26.95	22.38	0.44	15.12	5.24	0.45	0.80	0.54
CO	11.19	0.20	1.23	18.68	0.20	1.66	20.42	0.04	1.28
CO_2	2.35	9.72	11.07	2.81	10.90	19.57	1.48	37.72	22.46
H_2	31.25	8.70	19.02	49.08	22.33	61.16	46.82	61.08	71.09
H_2O	51.49	54.43	46.30	28.37	30.67	12.37	30.21	0.36	4.64

the reformer. Thus, the water−gas shift reaction is favored for the production of hydrogen at 723 K. However, the improvement in hydrogen production from the water−gas shift is too small to address the significant consumption of hydrogen by the methanation reaction. As a result, the yield of hydrogen at 723 K is very low (Figure 1).

At 823 K, the main product gases are methane (22.38 mol %), hydrogen (19.02 mol %), and carbon dioxide (11.07 mol %). The methanation reaction still dominates the reforming system, with the highest product methane content in the exit stream, except for the reactant steam. The water−gas shift reaction is also favored for the production of hydrogen with 11.07 mol % of carbon dioxide. Compared to the case at 723 K, the gas content of methane is 4.57 mol % lower; therefore, the steam reforming of methane becomes increasingly significant at the high temperature of 823 K, and more hydrogen is produced. In other words, at 823 K, the methanation reaction is suppressed. Because the methantion reaction is still the dominant reaction at 823 K, the yield of hydrogen at 823 K is still lower than that obtained at 623 K. Therefore, the nonmonotonic behavior of the hydrogen yield with respect to the reaction temperature is significantly affected not only by the thermodynamic equilibrium among the reversible reactions, but also by the relative importance of these competitive reactions in the range of temperatures investigated.

The reported yield of hydrogen from the steam reforming of heptane in a fixed bed reformer is about 2.0 at 723 K and 1489 kPa.[30] The simulated yield of hydrogen in this novel CFFBMR is around 2.4 at the same reaction temperature and pressure, which is the equilibrium yield of hydrogen. Both the experimental and simulation results show that the steam reforming system suffers from the thermodynamic equilibrium limitation for the production of hydrogen because of the reversible reactions, especially the strong methanation reaction for the steam reforming of higher hydrocarbons.

Isothermal CFFBMR Performance with Palladium-Based Hydrogen Membranes. In the following section, we investigate the effects of palladium-based hydrogen-selective membranes for both cocurrent and countercurrent configurations. The number of hydrogen-

permselective membranes is 10. The sweep gas in the hydrogen-permselective membranes is steam, and the operating pressure in the membranes is 101.3 kPa.

Cocurrent Operation. As discussed above, the production of hydrogen from the steam reforming of heptane suffers from the thermodynamic equilibrium barrier among the reversible reactions, especially from the methanation reaction. Because the methanation reaction is the reverse of the steam reforming of methane (second reaction in Table 1), the thermodynamic equilibrium limitations in the CFFBMR can be "broken" using hydrogen-permselective membranes. The removal of hydrogen decreases the partial pressure of hydrogen in the system, thereby enhancing the production of hydrogen. At normal operating conditions, the heptane steam reforming reaction is irreversible. Theoretically, the use of hydrogen-selective membranes should have no effect on the conversion of heptane. Figure 2 shows the simulated flow rate of heptane under cocurrent operation with 10 hydrogen permseletive membranes. Compared to the case without hydrogen-permselective membranes, which is shown in the same Figure 2, the flow rate of heptane at 623 K under cocurrent operation is higher near the entrance of the reformer and lower after the reactor length of 0.5 m. Moreover, the flow rates of heptane at 723 and 823 K also decrease faster with the membranes than without the membranes. This phenomenon can be explained using the kinetic rate equation for the steam reforming of heptane (first kinetic rate equation in Table 1). Chen et al.[1] found that the reaction rate for the steam reforming of heptane is nonmonotonic with respect to the partial pressure of hydrogen in the reaction side. That is, the rate of the steam reforming of heptane increased as the partial pressure of hydrogen in the reaction side increased from 0 to 25.33 kPa and then decreased as the partial pressure of hydrogen increased above 25.33 kPa. In most of the cases investigated, the partial pressure of hydrogen in the reaction side was above 25.33 kPa. Thus, the removal of hydrogen decreased the partial pressure of hydrogen in the reformer. Therefore, the rate of the steam reforming of heptane increased. As a result, the flow rate of heptane was lower with than without the hydrogen-permselective membranes. One might ask why the removal of hydrogen increases the rate of steam reforming of heptane when the partial pressure of hydrogen is higher than 25.33 kPa. This effect might occur because the removal of hydrogen decreases the chemisorbed fraction of hydrogen on the nickel catalyst surface. As a result, it increases the chemisoption of heptane on the catalyst surface and increases the reforming rate. In contrast, at low partial pressure of hydrogen (<25.33 kPa), the removal of hydrogen decreases the chemisorbed fraction of hydrogen on the catalyst, making the fraction of reduced nickel reforming catalyst smaller and, therefore, decreasing the reforming rate of heptane. Rostrup-Nielsen[20] suggested that the role of hydrogen in the reforming system is very complicated. Tottrup[21] has experimentally shown that increasing the flow rate of hydrogen increases the rate of steam reforming of heptane when the partial pressure of hydrogen in the reformer is around 5−21 kPa.

Table 4b shows the exit gas composition for the CFFBMR under cocurrent operations with 10 hydrogen membranes. The trend of the product gas composition

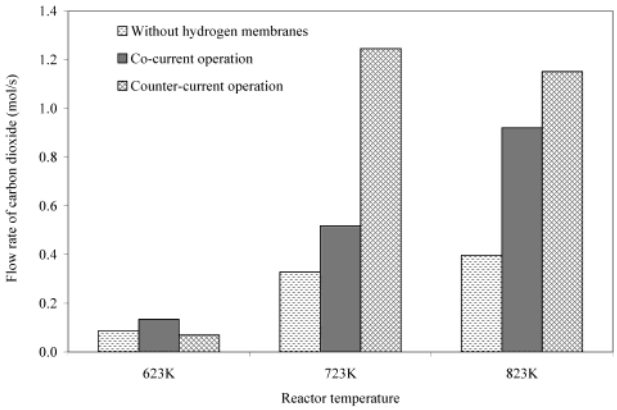

Figure 4. Flow rates of carbon dioxide in the CFFBMR under different operating conditions.

is similar to the case without hydrogen-permselective-membranes, except for the fact that much lower contents of methane and much higher contents of hydrogen are achieved at 723 and 823 K. As discussed earlier, at 623 K, the steam reforming of heptane is dominant in the system, and no thermodynamic equilibrium limits the reforming system because heptane is not fully converted. The content of methane at 623 K is 0.44 mol %. However, the contents of methane at 723 and 823 K are 15.12 and 5.24 mol %, respectively, which are much lower than the case without hydrogen-selective membranes (Table 4a). Thus, the content of methane in the exit gas stream is reduced by 43.90% at 723 K and by 76.59% at 823 K because of the use of hydrogen-permselective membranes. The removal of product hydrogen using hydrogen-selective membranes has suppressed the methanation reaction and increased the steam reforming of methane. Table 4b also shows that, at 723 K, the methanation reaction is still significant, even with hydrogen-permselective membranes. Figure 3 shows that the flow rate of methane at 723 K still increases along the reactor length after the full conversion of heptane, whereas at 823 K, it decreases. Thus, the removal of hydrogen broke the thermodynamic equilibrium limitation, and the steam reforming of methane was enhanced by the use of hydrogen-permselective membranes. Figure 4 shows the flow rates of carbon dioxide for different operation modes. Because carbon dioxide is mainly produced by the water−gas shift reaction in the reformer, the higher the flow rate of carbon dioxide, the larger the extent of the water−gas shift reaction. Using hydrogen-selective membranes, the removal of hydrogen shifts the reversible water−gas shift reaction toward the direction for hydrogen production, making the flow rate of carbon dioxide higher and the yield of hydrogen higher than the case without hydrogen-permselective membranes. For example, under cocurrent operation, the hydrogen yield is 12.95 at 623 K, 5.81 at 723 K, and 16.02 at 823 K, respectively. Compared with the cases without hydrogen-permselective membranes, the hydrogen yield is increased by 103.3, 287.3, and 335.3%, respectively. Undoubtedly, the CFFBMR performance is improved significantly through the use of hydrogen-permselective membranes.

Theoretically, if the hydrogen-permselective membranes are so efficient that any hydrogen produced in the reformer is "removed", then all of the reversible reactions can be considered as irreversible, and the steam reforming of heptane can be simplified by the

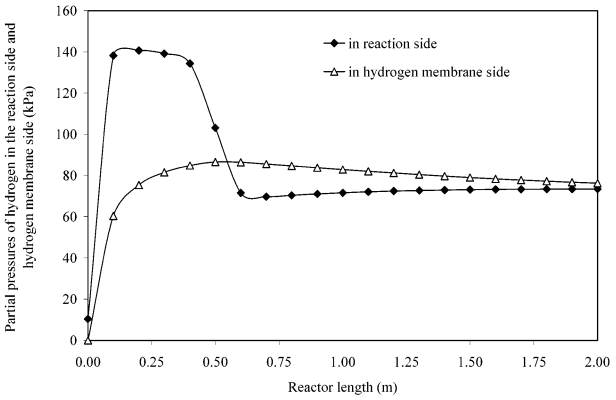

Figure 5. Partial pressures of hydrogen in the reaction side and hydrogen-permselective membrane side at 723 K under cocurrent operation.

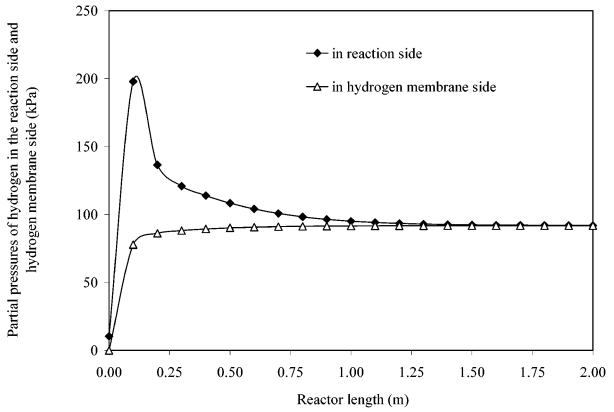

Figure 6. Partial pressures of hydrogen in the reaction side and hydrogen membrane side at 823 K under cocurrent operation.

following two irreversible reactions

$$C_7H_{16} + 7H_2O \rightarrow 7CO + 15H_2 \quad (4)$$

$$CO + H_2O \rightarrow CO_2 + H_2 \quad (5)$$

or by the overall irreversible reaction

$$C_7H_{16} + 14H_2O \rightarrow 7CO_2 + 22H_2 \quad (6)$$

Thus, the maximum yield of hydrogen is 22. When the yield of hydrogen obtained from the reforming system is lower than this value, there is still some room for further improvement.

As demonstrated earlier, the yield of hydrogen is significantly improved with hydrogen-permselective membranes under cocurrent operations. However, the yield of hydrogen is still nonmonotonic in relation to the reaction temperature, as shown in Figure 1. The yield of hydrogen at 723 K is much lower than the yields at other two temperatures 623 and 823 K. Further investigation shows that, at 723 K, the methanation reaction takes place continuously. As a result, the flow rate of methane at 723 K keeps increasing along the reformer length, as shown in Figure 3, which consumes a great deal of hydrogen. On the other hand, heptane is fully converted at the reactor length of 0.5 m (Figure 2). Then, beyond the reactor length of 0.5 m, the main contribution to hydrogen production by the steam reforming of heptane stops, meaning that the net production rate of hydrogen is negative along the rest of the reformer length. Because 3 mol of hydrogen is consumed for each 1 mol of methane formed during the fast methanation reaction, the consumption of hydrogen is so fast that the partial pressure of hydrogen in the reaction side decreases steeply, as shown in Figure 5. This steep drop makes the partial pressure of hydrogen in the reaction side suddenly lower than that in the membrane side. Therefore, back-permeation of hydrogen occurs, leading to a much lower yield of hydrogen at 723 K. However, at the temperature of 823 K, heptane is fully converted at the reactor length of 0.25 m (Figure 2). Then, the methanation reaction is suppressed because the main contribution of hydrogen through the steam reforming of heptane stops. On the other hand, the steam reforming of methane becomes increasingly important at 823 K as discussed earlier. As a result, the production of methane is changed to the situation of methane consumption, which makes the flow rate of methane decrease along the reactor length (Figure 3) after heptane full conversion at 0.25 m (Figure 2). Therefore, at 823 K, the yield of hydrogen is higher. The hydrogen produced from the steam reforming of methane (or the reverse of methanation) in the reaction side addresses the steep drop of the partial pressure of hydrogen, making the system better for the continuous removal of hydrogen (Figure 6). Thus, when hydrogen-permselective membranes are used, the hydrogen permeation driving force might also affect the hydrogen production. One can eliminate the problem of back-permeation at 723 K by increasing the flow rate of the sweep gas, steam, in the hydrogen membrane tubes. However, in this work, the velocity of the sweep gas in the membrane tubes was already high, and we kept it constant to meet the limitations for industrial practice and application.

Countercurrent Operation. As summarized in Table 2, countercurrent operation can be described as a two-point boundary value problem. In this paper, this problem is treated as a one-dimensional searching problem. Thus, one general optimization technique, the flexible tolerance optimization method (FTOM),[31] is used to solve this problem. One of the important advantages of using the FTOM optimization technique is the flexibility of using an adaptive step size for searching. The main idea is as follows: Given an initial guess for the hydrogen flow rate at the exit of the hydrogen membrane tubes, which is also the entrance of the reformer, the CFFBMR model is used to simulate the countercurrent operation. At the exit of the reformer or the entrance of the hydrogen membrane tubes, the simulated hydrogen flow rate in the hydrogen membrane tubes is compared to the initial boundary value for the hydrogen flow rate in the membrane tubes, which is zero in this case. If the simulated hydrogen flow rate is not zero, then the FTOM is used to optimize the searching direction and step size to find the solution. If the initial or new search guesses for the hydrogen exit flow rate in the membrane side are too small, then the solution obtained from the optimization could be a "false" solution, i.e., a solution with no physical meaning. To avoid this kind of false solution, Figure 7 is used to help to find the final right solution, which is plotted on the basis of a series of search data. For any initial guess of exit hydrogen flow rate, a flow rate of hydrogen at the entrance of the membrane tubes can be obtained. Then, the intercept on the x axis is the right solution; otherwise, the simulated "solutions" on the left side of this intercept are false solutions. Figure 7 also shows that the one-dimensional searching approach results in

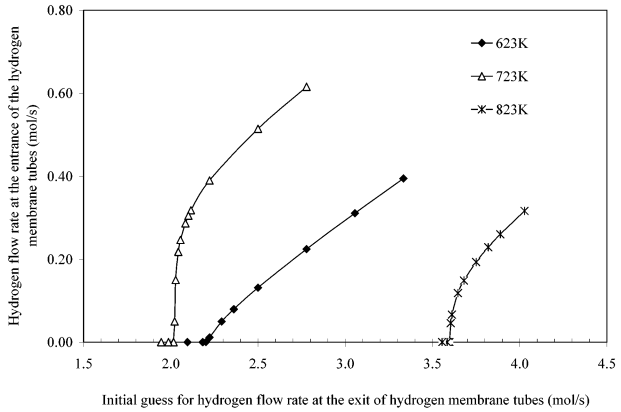

Figure 7. Schematic of the one-dimensional search process for the hydrogen flow rate at the exit of the hydrogen membrane tubes under countercurrent operation. (The intercept on the *x* axis is the right solution, whereas, the "solutions" on the left side of this intercept are false solutions.)

a stiff problem at 723 and 823 K, which makes the approach time-consuming and the search step size very small.

With the right solution for the two-point boundary value problem, the countercurrent operation in the CFFBMR was simulated at 623, 723, and 823 K. The yields of hydrogen for countercurrent operation are also shown in Figure 1. Similarly to the other two cases, the hydrogen yield is still nonmonotonic with respect to the reaction temperature. Table 4c shows the exit gas composition under countercurrent operation. The main differences between countercurrent and cocurrent operations are as follows: (1) The content of methane under countercurrent operation at 723 K is 0.80 mol %, whereas it is 15.12 mol % under cocurrent operation. (2) The content of carbon dioxide under countercurrent operation at 723 K is 37.72 mol %, whereas it is 10.90 mol % under cocurrent operation. (3) The content of hydrogen under countercurrent operation at 723 K is 61.08 mol %, whereas it is 22.33 mol % under cocurrent operation. In the steam reforming system, the lower concentration of methane and higher concentration of carbon dioxide mean a higher concentration of hydrogen. Thus, the yield of hydrogen at 723 K under countercurrent operation is much higher than the yields in the other two cases without hydrogen membranes and with hydrogen-permselective membranes under cocurrent operation. The reason for this improvement can be explained by the difference in the driving force for hydrogen permeation. As shown in Figures 5 and 6, there is a very small or negative differential partial pressure of hydrogen under cocurrent operation after heptane full conversion, so that the performance of the hydrogen-permselective membranes becomes inefficient and worse, for example, resulting in the back-permeation of hydrogen at 723 K. However, under countercurrent operation, the differential partial pressure of hydrogen between the reaction side and the hydrogen membrane side is larger, as shown in Figures 8 and 9 for 723 and 823 K, respectively. Under countercurrent operation, the differential partial pressure of hydrogen, the driving force for hydrogen permeation between the reaction side and hydrogen membrane side is positive along most of the reactor length. Thus, more product hydrogen is removed from the reformer, and a higher yield of hydrogen is obtained at 723 and 823 K. However, at 623 K, the removal of hydrogen under countercurrent operation slightly decreases the hydrogen yield. This is due to the back-permeation that occurs near the entrance of the reformer (or the exit of hydrogen-permselective membranes). Because the content of hydrogen in the feed is very small, at 623 K, the production rate of hydrogen is also very low. However, the content of hydrogen in the hydrogen-permselective membrane tubes is high. Thus, the negative differential partial pressure of hydrogen under countercurrent operation makes the final hydrogen yield slightly lower than the case under cocurrent operation. Figure 3 also shows the methane flow rate under countercurrent operation. The methane flow rate profile is much lower than in the other two cases, especially that at 723 K. Therefore, countercurrent operation provides a more promising engineering method to improve hydrogen production from the steam reforming of higher hydrocarbons. For countercurrent operation, the hydrogen yield is 12.13 at 623 K, 11.19 at 723 K, and 20.34 at 823 K. In contrast, under cocurrent operation, the hydrogen yield is 12.95 at 623 K, 5.81 at 723 K, and 16.02 at 823 K. The improvement for countercurrent operation from cocurrent operation is −0.063% at 623 K, 92.60% at 723 K, and 26.97% at 823 K.

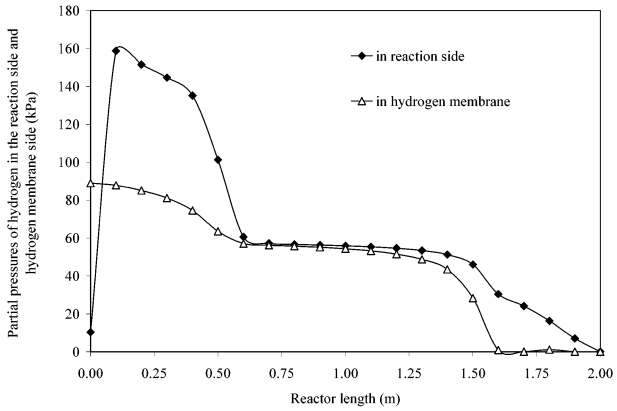

Figure 8. Partial pressures of hydrogen in the reaction side and hydrogen membrane side at 723 K under countercurrent operation.

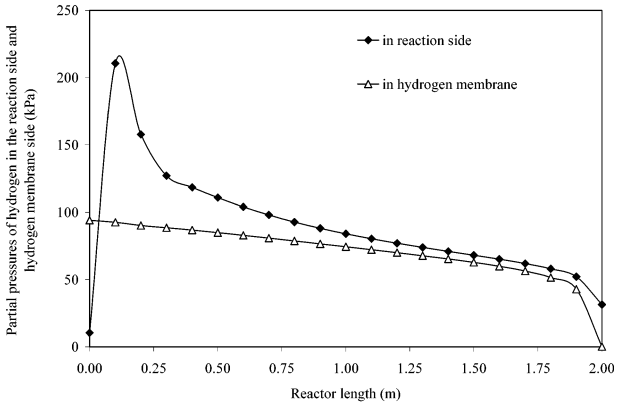

Figure 9. Partial pressures of hydrogen in the reaction side and hydrogen membrane side at 823 K under countercurrent operation.

Figure 2 shows that the highest hydrogen yield is obtained at 823 K for both cases with hydrogen-permeable membranes under cocurrent and countercurrent operations. Most of the product hydrogen permeated through the membranes is carried away by sweep gas, steam. Because steam can be condensed using a cooling agent such as cold water or cold saltwater, the final hydrogen purity can be estimated. For example, for cocurrent and countercurrent operations at 823 K, the simulated exit hydrogen concentra-

tion in the hydrogen-permselective membranes is 90.65 and 92.83 mol %, respectively. If the exit gases are further cooled to 300 K and most of the steam is condensed, the final hydrogen concentration can be as high as 99.45 and 99.59 mol %, respectively. Therefore, through the use of hydrogen-permselective membranes, the novel circulating fast fluidized bed membrane reformer has the potential to produce very pure hydrogen at high yield at normal operating conditions.

Conclusions

Using a mathematical model for the novel CFFBMR, the production of hydrogen from the steam reforming of higher hydrocarbons using heptane as a model hydrocarbon was investigated. The nonmonotonic behavior of the yield of hydrogen with respect to the reaction temperature was found to be due to the reaction characteristics and the thermodynamic equilibrium achieved during the steam reforming of heptane. When hydrogen-permselective membranes were used the driving force, the differential partial pressure of hydrogen between the reaction side and the membrane side also affected the permeation of hydrogen and, thus, the hydrogen production. Simulation results show that, without hydrogen-permselective membranes, at 623 K, the dominant reactions are the steam reforming of heptane and the water−gas shift reaction, whereas the methanation reaction and steam reforming of methane are not significant at this low temperature. At 723 K, the steam reforming of heptane is still the dominant reaction. However, after the full conversion of heptane, the methanation reaction dominates the system and consumes significant quantities of hydrogen, making the yield of hydrogen lower. However, at the higher temperature of 823 K, the steam reforming of methane becomes increasingly important, and the methanation reaction is suppressed. As a result, the yield of hydrogen is higher at 823 K than at 723 K. Nevertheless, the methanation reaction is still significant at 823 K, making the yield of hydrogen lower than that at 623 K. The simulation results also show that, at 723 and 823 K, the system suffers from the thermodynamic equilibrium limitation among the reversible reactions, especially from the methantion reaction. Using hydrogen-permselective membranes, the removal of hydrogen suppresses the formation of methane by the methanation reaction and encourages the steam reforming of methane and the water−gas shift reaction, leading to a higher yield of hydrogen. The methanation reaction is found to be still significant even with hydrogen membranes at 723 K. Further investigation found that back-permeation could occur in the reformer at 723 K under cocurrent operation because the methanation reaction consumes so much hydrogen, thereby steeply decreasing the partial pressure of hydrogen in the reaction side and producing a negative differential partial pressure of hydrogen between the reaction side and the hydrogen membrane side. As a result, the yield of hydrogen at 723 K is still lower than the yields at 623 and 823 K under cocurrent operation. Using countercurrent operation mode, the driving force of the differential partial pressure of hydrogen between the two sides becomes larger. This larger driving force enhances the reformer performance and improves the production of hydrogen, giving a higher hydrogen yield. The removal of hydrogen using hydrogen-permselective membranes "breaks" the thermodynamic equilibrium limitation among the reversible reactions. From the simulation results, it was found that, at low temperatures around 623 K, both cocurrent and countercurrent operations provide similar yields of hydrogen, whereas at the higher temperatures of 723 and 823 K, countercurrent operation provides the highest yield of hydrogen.

Acknowledgment

This work was financially supported by Auburn University, Grant 2-12085.

Symbols

a = index for cocurrent or countercurrent operation mode in model equation in Table 2
A = free cross-sectional area of the reactor (m^2)
d_{H_2} = diameter of the hydrogen membrane tubes (m)
E_i = activation energy of component i for reaction or permeation (J/mol)
F_i = molar flow rate of component i (mol/s)
k_j = the generalized reaction rate constant for the jth reaction
K_i = absorption constant for component i
K_j = reaction equilibrium constant for the jth reaction
l = reactor length (m)
L = total reactor length (m)
N_{H_2} = number of hydrogen membrane tubes
r_j = generalized reaction rate for the jth reaction [mol/($g_{catalyst}$ s)]
J_{H_2} = membrane permeation flux of hydrogen [mol/(m^2 s)]
J_i = membrane permeation flux of component i ($i \neq H_2$) [mol/(m^2 s)]
$\Delta H°$ = standard heat of reaction (J/mol)
P_i = partial pressure of component i (kPa)
Q = preexponential factor in the Arrhenius relationships for the permeability of hydrogen {J/[m s $(kPa)^{0.5}$]}
R = gas constant [8.314 J/(mol K)]
S/C = steam-to-carbon (of hydrocarbon) feed ratio (mol/mol)
T = temperature (K)

Greek Letters

δ_{H_2} = thickness of palladium-based hydrogen membranes (m)
ϵ = void fraction (v/v)
ρ_{cat} = density of solid catalyst (kg/m^3)
$\sigma_{i,j}$ = stoichiometric coefficient of component i in the jth reaction

Subscripts

i = reactants or products (i = C_7H_{16},CH_4, CO_2, CO, H_2, H_2O)
n = number of carbon atoms in a higher hydrocarbon molecule
m = number of hydrogen atoms in a higher hydrocarbon molecule
p = hydrogen membrane permeation side
r = reaction side
o = initial state or at the entrance of the reformer or membrane tube

Literature Cited

(1) Chen, Z.; Yan, Y.; Elnashaie, S. S. E. H. Modeling and Optimization of a Novel Membrane Reformer for Higher Hydrocarbons. *AIChE J.* **2003**, *49* (5), 1250−1265.

(2) Twigg, M. V. *Catalyst Handbook*, 2nd ed.; Wolfe Publishing Ltd.: New York, 1989.

(3) Christensen, T. S. Adiabatic Prereforming of Hydrocarbons—An Important Step in Syngas Production. *Appl. Catal. A* **1996**, *138*, 285−309.

(4) Adris, A. M.; Lim, C. J.; Grace, J. R. The Fluidized-Bed Membrane Reactor for Steam Methane Reforming: Model Verification and Parametric Study. *Chem. Eng. Sci.* **1997**, *52*, 1609−1622.

(5) Froment, G. F. Production of synthesis gas by steam- and CO_2- reforming of natural gas. *J. Mol. Catal. A* **2000**, *163*, 147−156.

(6) Hou, K.; Fowles, M.; Hughes, R. The Effect of Hydrogen Removal during Methane Steam Reforming in Membrane Reactors in the Presence of Hydrogen Sulphide. *Catal. Today* **2000**, *56*, 13−20.

(7) Elnashaie, S. S. E. H.; Adris, A. A Fluidized Bed Steam Reformer for Methane. In Proceedings of the International Fluidization *Conference, Banff, Canada; AIChE Publication 319; AIChE: New York, 1989.*

(8) Adris, A.; Elnashaie, S. S. E. H.; Hughes, R. Fluidized Bed Membrane Steam Reforming of Methane. *Can. J. Chem. Eng.* **1991**, *69*, 1061−1070.

(9) Hayakawa, T.; Andersen, A. G.; Shimizu, M.; Suzuki, K.; Takehira, K. Partial oxidation of methane to synthesis gas over some tibanates based perovskite oxides. *Catal. Lett.* **1993**, *22*, 307−317.

(10) Adris, A.; Grace, J.; Lim, C.; Elnashaie, S. S. E. H. Fluidized Bed Reaction System for Steam/Hydrocarbon Gas Reforming to Produce Hydrogen. U.S. Patent 5,326,550, 1994.

(11) Adris, A. M.; Lim, C. J.; Grace, J. R., The Fluidized Bed Membrane Reactor (FBMR) System: A Pilot Scale Experimental Study, *Chem. Eng. Sci.* **1994**, *49*, 5833−5843.

(12) Dyer, P. N.; Chen, C. M.; Bennett, D. L. Engineering Development of Ceramic Membrane Reactor Systems for Converting Natural Gas to Hydrogen and Synthesis Gas for Liquid Transportation Fuels, DE-FC26-97FT96052. In *Proceedings of the 1999 U.S. DOE Hydrogen Program Review*; NREL/CP-570--26938; U.S. DOE Washington, DC, 1999 (available at http://www.eere.energy.gov/hydrogenandfuelcells/pdfs/26938q.pdf).

(13) Dyer, P. N.; Chen, C. M. ITM Syngas and ITM H2: Engineering Development of Ceramic Membrane Reactor Systems for Converting Natural Gas to Hydrogen and Synthesis Gas for Liquid Transportation Fuels, DE-FC26-97FT96052. In *Proceedings of the 2000 U.S. DOE Hydrogen Program Review*; NREL/CP-570-28890; U.S. DOE: Washington, DC, 2000 (available at http://www.eere.energy.gov/hydrogenandfuelcells/pdfs/28890ww.pdf).

(14) Makel, D. B. *Low Cost Microchannel Reformer for Hydrogen Production from Natural Gas*; Project Report to the Energy Innovations Small Grant (EISG) Program; California Energy Commission (CEC): Sacramento, CA, 1999.

(15) Sammels, A. F.; Schwartz, M.; Mackay, R. A.; Barton, T. F.; Peterson, D. R. Catalytic Membrane Reactors for Spontaneous Synthesis Gas Production. *Catal. Today* **2000**, *56*, 325.

(16) Rostrup-Nielsen, J. Hydrogen via Steam Reforming of Naphtha. *Chem. Eng. Prog.* **1977**, *9*, 87−92.

(17) Aasberg-Petersen, K.; Bak Hansen, J. H.; Christensen, T. S.; Dybkjaer, I.; Seier Christensen, P.; Stub Nielsen, C.; Winter Madsen S. E. L.; Rostrup-Nielsen, J. R. Technologies for Large-Scale Gas Conversion. Appl. Catal. A: Gen. **2001**, *221*, 379−387.

(18) Phillips, T. R.; Mulhall, J.; Turner, G. F. The Kinetics and Mechanism of the Reaction between Steam and Hydrocarbons over Nickel Catalysts in the Temperature Range 350−500 °C, Part I. *J. Catal.* **1969**, *15*, 233−244.

(19) Bhatta, K. S. M.; Dixon, G. M. Role of Urania and Alumina as Supports in the Steam Reforming of *n*-Butane at Pressure over Nickel-Containing Catalysts. *Ind. Eng. Chem. Prod. Res. Dev.* **1969**, *8*, 324−331.

(20) Rostrup-Nielsen, J. R. Activity of Nickel Catalysts for Steam Reforming of Hydrocarbons. *J. Catal.* **1973**, *31*, 173−199.

(21) Tottrup, P. B. Evaluation of Intrinsic Steam Reforming Kinetic Parameters from Rate Measurements on Full Particle Size. *Appl. Catal.* **1982**, *4*, 377−389.

(22) Xu, J.; Froment, G. F. Methane Steam Reforming, Methanation and Water−Gas Shift: I. Intrinsic Kinetics. *AIChE J.* **1989**, *35* (1), 88−96.

(23) Elnashaie, S. S. E. H.; Elshishini, S. S. *Modelling, Simulation and Optimization of Industrial Fixed Bed Catalytic Reactors*; Gordon and Breach Science Publishers: London, 1993.

(24) Elnashaie, S. S. E. H.; Adris, A. M.; Al-Ubaid, A. S.; Soliman, M. A. On the Non-Monotonic Behaviour of Methane-Steam Reforming Kinetics. *Chem. Eng. Sci.* **1990**, *45* (2), 491.

(25) Kunni, D.; Levenspiel, O. Entrainment of Solids from Fluidized Beds: I. Hold-Up of Solids in the Freeboard; II. Operation of Fast Fluidized Beds, *Powder Technol.* **1990**, *61*, 193−206.

(26) Kunii, D.; Levenspiel, O. Circulating Fluidized-Bed Reactors. *Chem. Eng. Sci.* **1997**, *52* (15), 2471−2482.

(27) Shu, J.; Grandjean, B. P. A.; Kaliaguine, S. Methane Steam Reforming in Asymmetric Pd- and Pd−Ag/Porous SS Membrane Reactor. *Appl. Catal A* **1994**, *119*, 305−325.

(28) Barbieri, G.; Di Maio, F. P. Simulation of Methane Steam Reforming Process in a Catalytic Pd-Membrane Reactor. *Ind. Eng. Chem. Res.* **1997**, *36*, 2121−2127.

(29) *Pro Fortran: F90/F77/C/C++ Compilers and Tools*; Absoft Corporation: Rochester Hills, MI, 1999 (http://www.absoft.com).

(30) Phillips, T. R.; Mulhall, J.; Turner, G. F. The Kinetics and Mechanism of the Reaction between Steam and Hydrocarbons over Nickel Catalysts in the Temperature Range 350−500 °C, Part II. *J. Catal.* **1970**, *17*, 28−34.

(31) Himmelblau, D. M. *Applied Nonlinear Programming*; McGraw-Hill Book Company, New York, 1972; p 341.

Received for review December 13, 2002
Revised manuscript received September 19, 2003
Accepted September 19, 2003

IE021013J